An Experimental Validation of a Photovoltaic Emulator with Dual Loop PI Control for Accurate MPPT Testing

Machmud Effendy
Department of Electrical Engineering, University of Muhammadiyah Malang, Indonesia
machmud@umm.ac.id (corresponding author)

Khusnul Hidayat
Department of Electrical Engineering, University of Muhammadiyah Malang, Indonesia
khusnulhidayat@umm.ac.id

Ermanu Azizul Hakim
Department of Electrical Engineering, University of Muhammadiyah Malang, Indonesia
ermanuah@umm.ac.id

Received: 10 January 2026 | Revised: 5 February 2026 and 26 February 2026 | Accepted: 8 March 2026

 DOI: https://doi.org/10.48084/etasr.17464

ABSTRACT

This paper introduces a Photovoltaic Emulator (PVE) that uses a buck converter with dual-loop Proportional-Integral (PI) control to reliably test Maximum Power Point Tracking (MPPT) algorithms. The emulator utilizes a single-diode Photovoltaic (PV) model, solved using the Newton–Raphson method, to generate a reference current based on real-time voltage, irradiance, and temperature inputs. A dual-loop PI structure, consisting of an inner and outer current control loop, ensures accurate dynamic performance and stability. The proposed system was validated through simulations and experiments under various scenarios, including resistive load variations, irradiance and temperature changes, and integration with an MPPT converter. The results confirm that the emulator accurately reproduces the current-voltage (I-V) and power–voltage (P–V) characteristics of a PV module, enabling effective MPPT tracking with minimal steady-state error. This design offers a practical, reliable, and computationally efficient solution for laboratory-based PV system testing and MPPT algorithm evaluation.

Keywords-photovoltaic emulator; buck converter; maximum power point; PV cell model

I. INTRODUCTION

Solar energy is a renewable energy source that reduces dependence on fossil fuels. PV technology enables the direct conversion of sunlight into electricity, which can be used for applications ranging from household to large-scale power generation [1]. However, when conducted directly in the field, testing and developing PV systems, including MPPT algorithms, presents challenges. Weather variability, changes in solar irradiation, and other environmental factors lead to inconsistent and unreproducible test results. Therefore, a PVE is essential for replicating the I-V characteristics of PV panels under controlled, repeatable laboratory conditions [2-4]. Various approaches have been developed to construct reliable PVEs. Conventional methods use Proportional-Integral (PI) or Proportional-Integral-Derivative (PID) controllers with low bandwidth to suppress signal oscillations, resulting in slow dynamic responses [5-7]. Authors in [8] used the linear interpolation method and Boundary Control (BC)-based techniques, which provide faster responses but tend to be complex and require sophisticated control structures and dual-reference computations [9]. Authors in [10] proposed resistance feedback control based on a current-resistance (I-R) model, using binary search to achieve a fast dynamic response. However, this method relies on PI control and conventional buck converters, which have limitations in real-time response and are unstable under extreme loads. Alternative models have been developed to enhance PVE efficiency and response speed. These include PV cell-based models [11] and hybrid active-passive circuit topologies [12]. While these methods demonstrate improved performance, they still have drawbacks, including dynamic delays, increased component temperatures, and hardware complexity. PVEs using DC-DC converters controlled by sliding mode control algorithms have been implemented to replicate the I-V and P-V characteristics of actual PV modules. Nevertheless, these systems have issues, including dependency on mathematical models, limited measurement capacity, restricted dynamic response, and

hardware implementation complexity [13, 14]. Authors in [5, 15] proposed the single-diode model, which successfully replicates the I-V characteristics of PV panels with high accuracy but still encounters challenges, such as difficulty reproducing extreme curve conditions and a slow transient response. This study proposes a PV emulator that uses a buck converter controlled by a dual-loop PI controller. The emulator utilizes a single-diode PV model to generate a reference current based on the converter's output voltage via the Newton–Raphson method. This approach enables the emulator to converge quickly and track the operating point precisely under varying load conditions. Consequently, the emulator's dynamic response and steady-state accuracy are improved. Furthermore, the proposed framework enhances robustness against sudden changes in operating conditions while maintaining computational efficiency, controlling laboratory testing and the performance evaluation of MPPT algorithms and PV power conditioning systems. Overall, this study provides: real-time integration of a single-diode PV model with a cascaded dual-loop PI control architecture where the model's output current serves as the reference for enforcing PV behavior at the power stage, and a hierarchical control design that decouples fast electrical dynamics (the inner inductor current loop) from slower PV characteristic tracking (the outer PV current loop) to improve stability and transient performance.

II. PHOTOVOLTAIC MODEL

The electrical behavior of a PV cell can be described using the single-diode equivalent circuit shown in Figure 1. This circuit consists of a current source (I_{ph}) representing the photocurrent, a diode (D) to model the p-n junction, a series resistance (R_s) accounting for internal ohmic losses, and a parallel or shunt resistance (R_{sh}) representing leakage paths across the junction [16, 17].

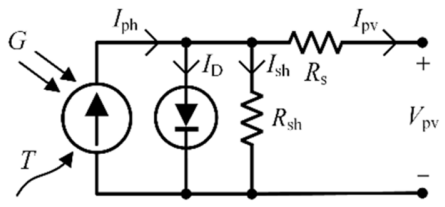

Fig. 1. Circuit representation of the single diode model.

Applying Kirchhoff's Current Law (KCL) to the output terminal of the PV cell, neglecting the small shunt leakage current I_{sh} due to the typically high value of R_{sh} in practical PV systems, leads to:

$$I_{pv} = I_{ph} - I_D \quad (1)$$

where I_{pv} is the output current, I_{ph} is the photocurrent, and I_D is the diode current. The current flowing through the diode follows the Shockley diode equation:

$$I_D = I_0 \left(exp \left(\frac{V_{pv}+I_{pv}R_s}{N_s V_t} \right) - 1 \right) \quad (2)$$

where V_{pv} is the terminal voltage, I_0 is the diode reverse saturation current, R_s is the series resistance (internal losses), N_s is the number of PV cells connected in series, and V_t is the thermal voltage. The thermal voltage V_t is a function of the junction temperature:

$$V_t = \frac{nkT_k}{q} \quad (3)$$

where n is the diode ideality factor (n = 1.2 for Monocrystalline silicon) [2], $k = 1.381 \times 10^{-23}$ J/K is Boltzmann's constant, $q = 1.602 \times 10^{-19}$ C is the electron charge, and T_k is the PV cell temperature in Kelvin. Substituting the diode current into the KCL (1) gives a non-linear implicit equation for the terminal current I_{pv}:

$$I_{pv} = I_{ph} - I_0 \left(exp \left(\frac{V_{pv}+I_{pv}R_s}{N_s V_t} \right) - 1 \right) \quad (4)$$

The non-linear nature of (4) requires a numerical solution. The Newton–Raphson method is chosen due to its quadratic convergence and efficiency. The iterative formula used is:

$$f(I_{pv}) = I_{pv} - I_{ph} + I_0 \left(exp \left(\frac{V_{pv}+I_{pv}R_s}{N_s V_t} \right) - 1 \right) \quad (5)$$

$$f'(I_{pv}) = 1 + I_0 \, exp \left(\frac{V_{pv}+I_{pv}R_s}{N_s V_t} \right) \cdot \frac{R_s}{N_s V_t} \quad (6)$$

The initial PV current is initialized as $I_{pv} = I_{ph}$, assuming that the diode and series resistance effects are initially negligible. The current is updated iteratively as:

$$I_{pv,new} = I_{pv,old} - \frac{f(I_{pv})}{f'(I_{pv})} \quad (7)$$

To ensure convergence without excessive computation, the Newton–Raphson iteration is limited to a maximum of 10 steps. Additionally, the iterative process terminates early if the difference between successive current estimates ($I_{pv,new} - I_{pv,old}$) falls below the predefined threshold of 10^{-6}, which indicates sufficient convergence.

III. SYSTEM CONFIGURATION AND CONTROL ARCHITECTURE

The proposed system configuration consists of a DC voltage source connected to a two-stage power conversion system, as shown in Figure 2. The first stage is a buck converter configured as a PWM, and the second stage is a buck converter that implements MPPT. A resistive load is connected to the MPPT stage's output. The PVE emulates the electrical behavior of a PV module by adjusting its output current (I_{pv}) based on the terminal voltage (V_{pv}), using a single-diode PV model. A dual-loop PI control strategy is applied. The outer loop regulates the PV output current (I_{pv}) to follow the reference current ($I_{pv,\,ref}$) from the PV model. The inner loop controls the inductor current (I_L) to ensure a fast response and stable current tracking. The resulting duty cycle is applied to the PVE switch via a Pulse Width Modulation (PWM) generator. An LC filter is placed between the PVE and MPPT stages to attenuate switching ripple and decouple the dynamics of the two converters. The MPPT stage not only provides MPPT functionality but also serves as a test platform to validate the dynamic and steady-state behavior of the proposed PVE under varying operating conditions. The MPPT stage adjusts its duty cycle based on V_{pv} and I_{pv} measurements, ensuring optimal power delivery to the resistive load. In addition to MPPT functionality, this stage provides a realistic,

controllable environment to evaluate the dynamic and steady-state performance of the proposed PV emulator under varying operating conditions. The proposed system uses the Perturb and Observe (P&O) algorithm to perform MPPT in real time. The MPPT algorithm is implemented as a discrete-time task on the microcontroller and is synchronized with the Analog-to-Digital Converter (ADC) sampling and PWM update cycle.

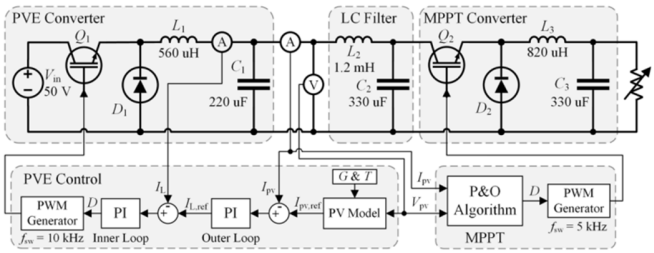

Fig. 2. Block diagram of the proposed system including PV emulator, MPPT converter, and control subsystems.

IV. SIMULATION RESULTS AND DISCUSSION

To verify the proposed PVE, the emulator was simulated in MATLAB/Simulink and validated through hardware creation in-loop.

A. Simulation Verification

The test was performed using MATLAB/Simulink with the PVE model parameters listed in Table I, and was evaluated under two test scenarios.

TABLE I. PV MODEL PARAMETERS

Parameters	Values	Parameters	Values
N_s	60	β_{Voc}	-0,369 %/°C
$V_{oc,ref}$	37.3 (V)	α_{Isc}	0,092 %/°C
$I_{sc,ref}$	8.66 (A)	R_s	0.01 (Ω)

1) Scenario 1: PV Emulator I–V Characteristics

The first simulation scenario was conducted to evaluate the PV emulator's ability to replicate a PV module's I–V characteristics under varying environmental conditions. This scenario consists of two subtests: one examining the effect of irradiance changes at a constant temperature and the other examining the effect of temperature changes at a constant irradiance, as presented in Figure 3.

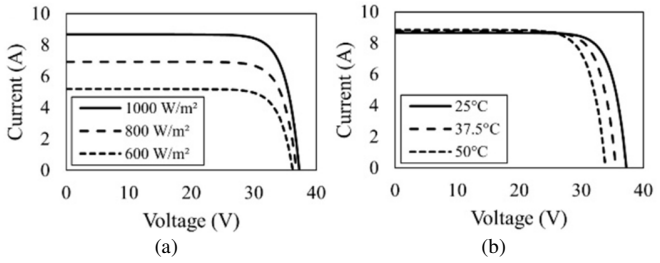

Fig. 3. I–V characteristics for: (a) different insulations and (b) different temperatures.

Figure 3 (a) depicts the I–V characteristics of the PV emulator at different irradiance levels (1000 W/m², 800 W/m², and 600 W/m²) while maintaining a constant temperature of 25 °C. As expected, the short-circuit current (I_{sc}) decreases significantly with a reduction in irradiance. The open-circuit voltage (V_{oc}) exhibits only slight variation. This behavior is consistent with the theoretical model of PV modules, indicating that the emulator accurately reproduces the response of a real PV panel to changes in irradiance. Figure 3 (b) demonstrates how temperature variation impacts the I–V characteristics when the irradiance is kept constant at 1000 W/m², and the temperature is varied from 25°C to 50°C. As the temperature increases, the open-circuit voltage (Voc) decreases while the short-circuit current (I_{sc}) remains nearly unchanged. This matches the typical behavior of a PV module, where an increase in temperature results in reduced efficiency due to a decrease in V_{oc}.

2) Scenario 2: MPPT Performance under Irradiance Variation

The second simulation scenario evaluates the dynamic performance of the PV system when connected to a DC-DC converter that implements the P&O MPPT algorithm. The converter is connected to a 2 Ω resistive load. During the simulation, the irradiance input to the PVE is varied to test the system's ability to track the Maximum Power Point (MPP) in real-time. Initially, the irradiance is set at 1000 W/m². It then drops to 600 W/m² at 1.5 s and increases to 800 W/m² at 2.5 s. The results are presented in Figure 4, consisting of three subplots showing the PVE's power, voltage, and current responses, along with their corresponding MPP references (P_{max}, V_{mpp}, and I_{mpp}). Figure 4 (a) shows that the PVE's output power (P_{pv}) closely tracks the maximum available power (P_{max}) across all irradiance levels. Although transient deviations occur immediately after each irradiance change, the P&O algorithm successfully adjusts the converter's duty cycle, restoring operation near the new MPP. This is particularly evident during steady-state conditions, when P_{pv} and P_{max} are nearly identical. Figure 4 (b) displays the PVE voltage (V_{pv}) following the MPP voltage reference (V_{mpp}). When irradiance changes, a brief mismatch occurs due to the nature of the P&O algorithm; however, the controller quickly converges to the correct operating point. The emulator's ability to produce the correct voltage profile reinforces the effectiveness of the voltage control loop within the emulator system. Based on Figure 4 (b), the voltage control loop exhibits a fast transient response, with an estimated rise time of approximately 0.2 s, following irradiance-induced disturbances. A small overshoot of about 4% is observed during step increases in the reference voltage. In steady-state operation, the tracking error between the emulator output voltage (V_{pv}) and the reference MPP voltage (V_{mpp}) remains below 0.5%, indicating high steady-state accuracy and stable voltage regulation. Figure 4 (c) illustrates the current response (I_{pv}) compared with the ideal MPP current (I_{mpp}). Similar to the voltage and power plots, the current closely follows the MPP target with minimal error during steady-state conditions and acceptable transients during irradiance shifts.

B. Experimental Verification

The proposed system configuration is implemented in hardware to integrate the PVE and MPPT converters. Each converter has its own embedded controls in a 32-bit ARM Cortex-M microcontroller that operates at 168 MHz.

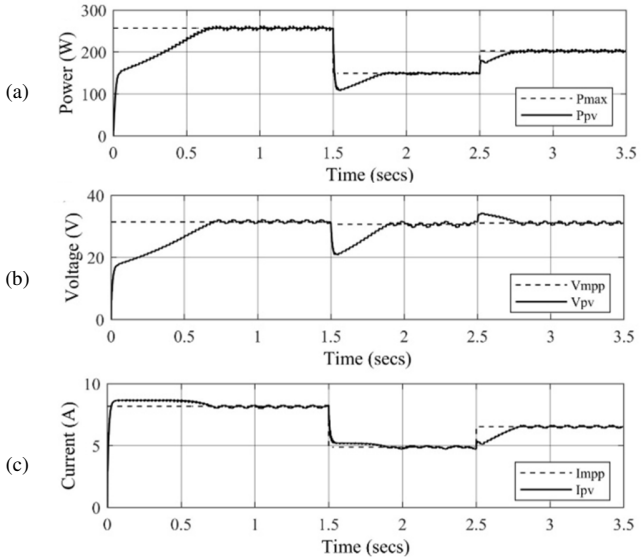

Fig. 4. PVE response under varying irradiance with MPPT load: (a) power, (b) voltage, (c) current.

The device integrates multiple 12-bit ADC channels for synchronous sampling of V_{pv}, I_{pv}, and I_L, and advanced timer modules that can generate high-resolution PWM signals for the PV emulator and MPPT converter. The Cortex-M4 core's computational capability enables real-time execution of the Newton–Raphson PV model, dual-loop PI control, and the P&O MPPT algorithm within a single control cycle, as portrayed in Figure 5. The converter parameters used are listed in Table II. To validate PVE performance, experiments were conducted through two scenarios.

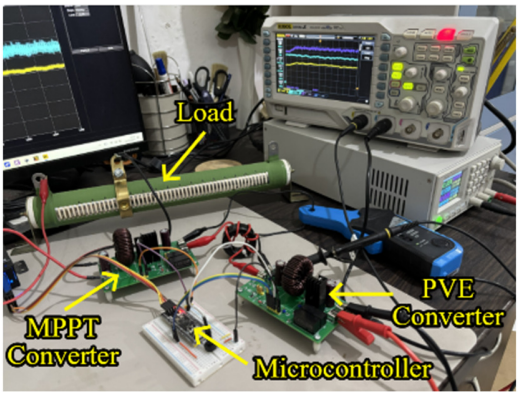

Fig. 5. Hardware settings.

1) Scenario 1: PV Emulator I–V Characteristics

This experiment evaluates the ability of the PV emulator to replicate the I–V characteristics of a PV module during irradiation and temperature fluctuations. Figure 6 shows the I–V characteristics, comparing the simulated and experimental results of PV modules at various irradiance levels and temperatures. The output current decreases proportionally with irradiance, while the voltage remains nearly constant until reaching the open-circuit region. Conversely, as temperature increases, the open-circuit voltage decreases while the current remains nearly constant, resulting in reduced output power. The similarity between the simulated and experimental curves validates the accuracy of the proposed PV model in representing real-world module performance under different solar conditions.

TABLE II. PARAMETERS OF CONVERTERS

Converter	Parameters	Symbol	Values
PVE converter	Rated power	P_m	300 (W)
	Voltage input	V_{in}	40 (V)
	Frequency switching	f_{sw}	25 (kHz)
	Inductor	L	100 (µH)
	Capacitor	C	470 (µF)
MPPT converter	Rated power	P_m	300 (W)
	Voltage input	V_{in}	37.3 (V)
	Frequency switching	f_{sw}	12.5 (kHz)
	Inductor	L	120 (µH)
	Capacitor	C	470 (µF)

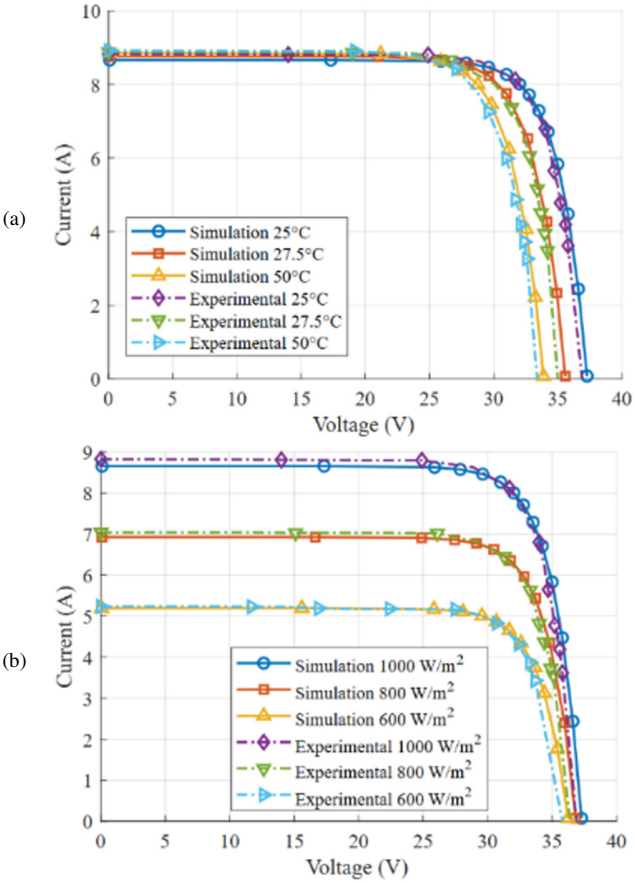

Fig. 6. Experimental results of I–V characteristics for: (a) irradiation fluctuations, (b) temperature changes.

2) Scenario 2: MPPT Performance

The second experiment validated the performance of the PVE when connected to a DC-DC converter that used the P&O MPPT algorithm. This experiment used a 2 Ω resistive load and a temperature of 25°C. The applied irradiance was 1000 W/m², 800 W/m², and 600 W/m², respectively. Figure 7 presents the power-voltage characteristics of the PV system under simulated and experimental conditions. The curves are similar in shape and have nearly identical maximum power points (P_{max}). Table III summarizes the simulation and experimental results for three types of irradiances.

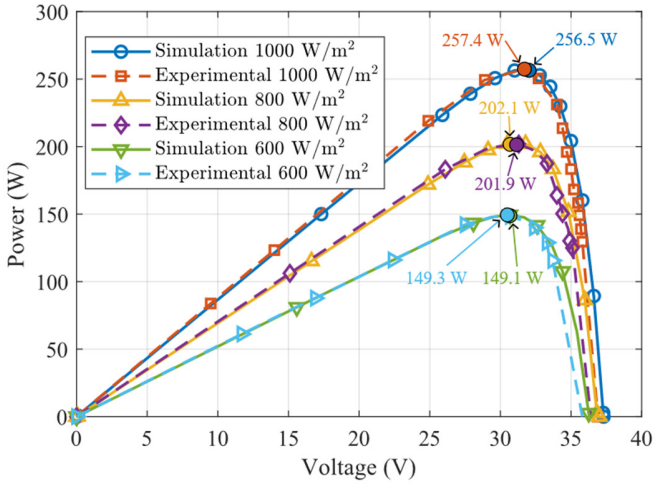

Fig. 7. Experimental results of P–V characteristic.

TABLE III. COMPARISON OF MPPT PERFORMANCE TESTING UNDER VARYING IRRADIANCES

Irradiance (W/m²)	Power (W)		Similarity (%)
	Simulation results	Experimental results	
600	149.1	149.3	99.9
800	202.1	201.9	99.9
1000	256.5	257.4	99.6

V. CONCLUSIONS

This study presented the design of a Photovoltaic Emulator (PVE) system using a buck converter with dual-loop Proportional-Integral (PI) control. The proposed system employs a single-diode Photovoltaic (PV) model and the Newton–Raphson method to generate a reference current based on the converter's output voltage. The dual-loop PI controller ensures accurate tracking of PV characteristics. The system was tested under various load conditions, including resistive loads and Maximum Power Point Tracking (MPPT) converter loads. The proposed PVE was simulated and tested in a laboratory setting. The simulation results demonstrate that the proposed PVE can replicate PV behavior with high accuracy and dynamic performance. When tested with resistive loads, the emulator consistently matched the reference current-voltage (I-V) and power–voltage (P–V) curves across varying levels of solar irradiance and temperature. When tested with an MPPT converter load, the emulator successfully responded to changes in irradiance, enabling the MPPT algorithm to effectively track the maximum power points (P_{max}). These results suggest that the proposed approach is suitable for testing PV systems and MPPT algorithms in controlled environments. The experimental results show that the I-V characteristics of the PV and the MPPT performance of the PVE are identical to the simulation results. The average percentage similarity for MPPT performance is 99.8%. Further research could evaluate MPPT algorithms in more realistic scenarios by including partial shading and multi-peak PV models.

ACKNOWLEDGMENT

The authors would like to express their gratitude to the Indonesian Ministry of Higher Education, Science, and Technology for funding this research. They also thank the Institute for Research and Community Service, University of Muhammadiyah Malang, for its continued support.

REFERENCES

[1] M. Effendy, M. Ashari, and H. Suryoatmojo, "PV generation–energy storage coordination with adaptive droop control in isolated DC microgrid," *International Journal of Innovative Computing, Information and Control*, vol. 19, no. 3, pp. 655–669, 2023, https://doi.org/10.24507/ijicic.19.03.655.

[2] A. Boucharef, A. Tahri, F. Tahri, S. Silvestre, and M. Bourahla, "Solar module emulator based on a low-cost microcontroller," *Measurement*, vol. 187, 2022, Art. no. 110275, https://doi.org/10.1016/j.measurement.2021.110275.

[3] V. M. Cavalcante Junior, R. C. Neto, E. J. Barbosa, F. Bradaschia, M. C. Cavalcanti, and G. M. S. de Azevedo, "Evaluation of the effectiveness of solar array simulators in reproducing the characteristics of photovoltaic modules," *Sustainability*, vol. 16, 2024, Art. no. 6932, https://doi.org/10.3390/su16166932.

[4] I. Moussa, A. Khedher, and A. Bouallegue, "Design of a low-cost PV emulator applied for photovoltaic energy conversion systems," *Electronics*, vol. 8, no. 2, 2019, Art. no. 232, https://doi.org/10.3390/electronics8020232.

[5] A. S. Samosir, H. Gusmedi, and A. F. Huda, "Design and implementation of PV emulator based on synchronous buck converter using Arduino Nano microcontroller," *International Journal of Power Electronics and Drive Systems*, vol. 16, no. 1, pp. 448–456, 2025, https://doi.org/10.11591/ijpeds.v16.i1.pp448-456.

[6] Krismadinata, S. Anggraini, Asnil, R. Mulya, Syafii, and Fahmi, "Design and implementation of photovoltaic emulator for testing of photovoltaic energy conversion system," *SSRG International Journal of Electrical and Electronics Engineering*, vol. 12, no. 4, pp. 191–200, 2025, https://doi.org/10.14445/23488379/IJEEE-V12I4P113.

[7] A. Ramyar and A. T. Avestruz, "Reconfigurable photovoltaic emulator for differential diffusion charge redistribution solar modules," *IEEE Open Journal of Industry Applications*, vol. 2, pp. 36–46, 2021, https://doi.org/10.1109/OJIA.2021.3063842.

[8] L. Q. Thai and A. T. H. T. Anh, "Design a photovoltaic simulator system based on two-diode model with linear interpolation method," *International Journal of Power Electronics and Drive Systems*, vol. 13, no. 2, pp. 856–864, 2022, https://doi.org/10.11591/ijpeds.v13.i2.pp856-864.

[9] I. D. G. Jayawardana, C. N. M. Ho, M. Pokharel, and G. E. Valderrama, "A fast-dynamic control scheme for a power-electronics-based photovoltaic emulator," *IEEE Journal of Photovoltaics*, vol. 11, no. 2, pp. 485–495, 2021, https://doi.org/10.1109/JPHOTOV.2020.3041188.

[10] H. A. Khawaldeh, M. Al-Soeidat, D. D.-C. Lu, and L. Li, "Simple and fast dynamic photovoltaic emulator based on a physical equivalent PV-cell model," *The Journal of Engineering*, vol. 2021, no. 5, pp. 276–285, 2021, https://doi.org/10.1049/tje2.12032.

[11] H. A. Khawaldeh, M. Al-Soeidat, M. Farhangi, D. D.-C. Lu, and L. Li, "Efficiency improvement scheme for PV emulator based on a physical

equivalent PV-cell model," *IEEE Access*, vol. 9, pp. 83929–83939, 2021, https://doi.org/10.1109/ACCESS.2021.3086498.

[12] H. A. Khawaldeh, M. Al-Soeidat, D. D.-C. Lu, and L. Li, "Accurate, fast and power efficient PV emulator based on hybrid passive and active circuits," *CPSS Transactions on Power Electronics and Applications*, vol. 7, no. 4, pp. 432–441, 2022, https://doi.org/10.24295/CPSSTPEA.2022.00039.

[13] M. Chaker, A. El Houre, D. Yousfi, M. Kourchi, M. Ajaamoum, H. Idadoub, and J. Bouchnaif, "Development of a PV emulator using SMPS converter and a model selection mechanism for characteristic generation," *Solar Energy*, vol. 239, pp. 117–128, 2022, https://doi.org/10.1016/j.solener.2022.04.049.

[14] P. Korasiak and J. Jaglarz, "A new photovoltaic emulator designed for testing low-power inverters connected to the LV grid," *Energies*, vol. 15, no. 7, 2022, Art. no. 2646, https://doi.org/10.3390/en15072646.

[15] A. Gholami, M. Ameri, M. Zandi, and R. Gavagsaz Ghoachani, "A single-diode model for photovoltaic panels in variable environmental conditions: Investigating dust impacts with experimental evaluation," *Sustainable Energy Technologies and Assessments*, vol. 47, 2021, Art. no. 101392, https://doi.org/10.1016/j.seta.2021.101392.

[16] Z. Song *et al.*, "An Effective Method to Accurately Extract the Parameters of Single Diode Model of Solar Cells," *Nanomaterials*, vol. 11, no. 10, Oct. 2021, Art. no. 2615, https://doi.org/10.3390/nano11102615.

[17] H. A. Ismail and A. A. Z. Diab, "An efficient, fast, and robust algorithm for single diode model parameters estimation of photovoltaic solar cells," *IET Renewable Power Generation*, vol. 18, no. 5, pp. 863–874, 2024, https://doi.org/10.1049/rpg2.12958.